RSC Advances

ROYAL SOCIETY OF CHEMISTRY

www.rsc.org/advances

In vivo detection of fluoride at trace level and its removal from raw water at neutral pH utilizing cyanobacterium pigment as a luminescent probe

Mousumi Chatterjee, Chandan Ghosh, Milan K. Barman, Bhavya Srivastava, Dipika Roy and Bhabatosh Mandal*

Department of Chemistry, Visva-Bharati, Santiniketan-731235, India

E-mail: bhabatosh_mandal@yahoo.co.in

Abstract: A selective method has been developed for trace level (0.01 mg L^{-1}) fluoride detection in hepes buffer in presence of interfering ions (like Cl^-, I^-, Br^-, SO_4^{2-}, ClO_4^-, CH_3COO^-) using cyanobacterium as a **luminescent probe**. It is well below PHS recommended levels for drinking water (0.7−1.2 ppm), placing this probe among the most subtle fluoride sensors reported to date. Cellular pigments, Phycocyanobilin2 of living algae play an anchoring role to sense fluoride at trace level by an instantaneous fluorescence. Algal bio mass was used for removal of fluoride from raw water at neutral pH. Maximum uptake capacity (BTC: 6.76 mg g^{-1}; Q_0: 6.08 mg g^{-1}) and preconcentration factor (PF: 64.2) were found to be appreciably high. Interference caused by the presence of several co-existing ions has been discussed. The proposed method has been applied on real samples like pond water, well water and ground water with good analytical reliability such as removal of fluoride up to 92.3±1.3 %, with a relative standard deviation of 2-3%, and re-usability of 70-90 cycles.

1. INTRODUCTION:

Presently research on receptors and sensors for anions is attracting much interest because of the importance of anions in environmental, biological, and chemical processes [1]. Fluoride intake is always regarded as a double-edged sword. On one hand, fluoride plays a beneficial role in treating osteoporosis and protecting dental health [2]; on the other hand, excessive ingestion of fluoride may cause fluorosis

[3] and urolithiasis [1, 4]. Fluorosis caused by high fluoride concentrations (>1.5 mg L^{-1}) has been reported in various countries including India, Argentina, UK, South Africa, the United States, Norway, Mexico, China, and Poland [3,4]. Fluoride toxicity leads to enhanced bone density and cancer [5]. Due to these adverse and beneficial effects of fluoride the development of sensor for trace level fluoride detection has fascinated many researchers [6]. Till date, most of the reported and common sensor designs involve polarization of the –NH protons in heterocyclic nitrogen pyrrole and indole moieties [6], or in urea / thiourea / pyrrole / amide and imidazolium [7] moieties, where design strategies are mostly sophisticated, expensive and sometimes exhibit delayed response for a particular recognition event [7]. And, these developed fluoride sensors mainly worked with one of the following strategies such as anion–π interactions [8], fluoride-hydrogen bonding at –NH proton [6, 9], irreversible cleavage of O–Si bond [10] and Lewis acid–base interaction (boron-fluoride complexation) [11]. These methods have disadvantages like (a) formation of B–F bond in tri-coordinated organoboron which has interference of cyanide and (b) the interference of fluoride assisted cleavage of Si–O bond by thiols [12]. Rhodamine imidazole derivative has recently been utilized for fluorescence imaging of fluoride in HeLa cells under physiological conditions [13]. Herein, we report the design of a biosensor based on algal pigment (present inside the living cyanobacterium) appended Rhodamine B dye that enables the trace level detection of fluoride ions in vivo selectively. It goes without saying that along with trace level detection, removal of fluoride in real samples poses a challenge to analytical chemists. The fluoride contamination control in groundwater is difficult since fluoride contamination is influenced by many hydrogeologic and physicochemical parameters [14]. Defluoridation methods have been critically reviewed [15, 16]. Adsorption is now evolving as a front line of defense. Selective adsorption utilizing titanium-rich bauxite [17], various forms of quartz [18], aluminum sorbent [19], aluminum-impregnated carbon [20], activated alumina [21], alum-impregnated activated alumina [22], aluminum-type superparamagnetic adsorbents

[23], activated carbons (ACs), carbon black [24], red mud [25], zeolite [26], chitin and chitosan [27], magneticchitosan particle [28], lime stone [29], biomass and carbonized biomass [30], carbonaceous materials [31], and bone char [32] were reported. Metabolic specificity for a given toxicant can be advantageous in bioremediation strategies in bioaccumulation [33, 34]. Biosorption offers a potential alternative to conventional processing methods, mainly because of their low cost, strong metal binding capacity, high sorption efficiency in dilute effluents, environmental friendliness and, more importantly, because of their self maintained adsorbent beds [33, 34]. Besides, it provides a cost-effective solution for industrial wastewater management [35]. In the present study, the analytical applicability of Phormidium luridum (microalgae) as a biosorbent and biosensor for the detection/recovery/removal of fluoride has been rationalized for following reasons. Firstly, the toxicant is of high concern and attracting a mounting interest in the scientific community due to its duplicitous nature (used in human diet, drinking water should contain $\leq$ 1.5 mg L^{-1} but, recently it has been accused for several human pathologies) [2-6]. Secondly, limited number of studies was available on the treatment by algal species (fresh and marine water) in spite of their ubiquitous distribution and their central role in the fixation and turnover of carbon [36, 37]. Moreover, this potential biosorbent can easily intake fluoride inside its living cell [38].

Our present study advocates a selective, rapid, eco-friendly and cost-effective method for the detection, preconcentration, separation, recovery and removal of aqua fluoride-species (asymm.) from aqueous solution of a complex nature (comprising of coexisting ions in concentration ranges similar to their natural abundance) at near neutral pH (6.5–6.8) by cyanobacterium. More importantly, global hardness (η) is a definite quantum mechanical descriptor and is the cardinal index of chemical reactivity, as well as the stability of atoms and ions [39]. A standard Density Functional Theory (DFT) [40] calculation has thus been performed, not only to analyze the structure of the extractor site and the extractor–[(assym. HF_2^-(aq)] complex, but also to rationalize the sorption pathway in terms of hardness.

2. EXPERIMENTAL:

2.1. Apparatus and reagents: Olympus BX41 epifluorescence trinocular microscope fitted with digital camera, Nikon Coolpix 4500 at a magnification of 45×10 was used to identify the specific algal strain. Fluorescence micrographs were recorded on Leica (model no: Leica DM1000, Germany) fitted with a digital camera (Leica DF420C), at a magnification of 45× 10 utilizing LAS (Leica Application Suite) Software (Version 4.1.0) at its experimental conditions as follows: Left part (A): excitation (UV source), excitation filter (BP340-380), Mirror (400), Suppression (LP425); Middle part (I_3): excitation (Blue source), excitation filter (BP450-490), Mirror (510), Suppression (LP515); Right part: excitation (Green source), excitation filter (BP515-560), Mirror (580), Suppression (LP590). Confocal microscopy images were taken on LEICA TCS SP8 inverted microscope with LASX Software using 405 nm laser sources for excitation. The pH measurements were carried out with a digital Elico L1-120 pH meter combined with glass electrode. The scanning electronic microscopy (SEM) image for the algae was obtained at 15 KV by S530 HETACHI, Japan. Fourier transform infrared (FTIR) spectra of the biosorbent in its F^- loaded and unloaded forms were recorded in the range of 4500–500 cm^{-1} on Shimadzu FTIR spectrophotometer (Model no FTIR – 8400S) using sample : KBr pellets in the weight ratio 1 : 10. The amount of fluoride was estimated by an ion selective electrode, Thermo Scientific (Orion 5 Star Benchtop Multi W/ISE mtr, Singapore). A thermostat was used to carry out the extraction under the controlled temperature. Different salt solutions were prepared by dissolving NaCl, $NaNO_3$, NaH_2PO_4 and NaF in distilled water. All of these chemicals and solvents used in this work, unless otherwise stated, were of analytical grade (BDH, Mumbai, India /E Merck, Mumbai, India). A perkinElmer LS-55 spectrofluorometer was used to carry out the fluorescence titration experiments.

2.2. Identification of algae: Axenic culture of the green microalgae, P. luridum, originally isolated from a soil sample, collected from river basin, Ajoy [33, 34] and maintained in the Analytical

Laboratory, Department of Chemistry, Visva-Bharati, was used in this study. An aliquot of culture was grown in 100 mL Erlenmeyer flasks containing 25 mL of BG 11 (+)[33, 34] in an orbital shaker set at 150 rpm under 3 × 36 W cool white fluorescent light at 24 ± 2°C [41]. P. luridum was identified [15] within three days of its collection without fixation by comparing various standard monographs with our microscopic observation using an Olympus BX41 epifluorescence trinocular microscope.

2.3 Trace level detection of fluoride: Fluorescence micrographs were recorded to observe any transport of fluoride inside the living cell. The cultures were examined in microscope for the presence of any contaminating fluorescent materials or debris in the medium other than the autofluorescent microalgal cells. After staining with Rhodamine B, algal cells were exposed to fluoride to observe its effect on the fluorescent pattern for Rhodamine B. The micrographs were taken at 10, 15 and 20 minutes of incubation with fluoride of fixed concentration (0.01 mg mL^{-1}). The micrographs were also taken at fixed time interval (10 minutes) of incubation with different initial fluoride concentrations (0.01-0.1 mg L^{-1}). Same investigations were also performed with the algal cells; either having no Chlorophyll-a or containing completely damaged Chlorophyll-a to find out the role of this pigment behind any kind of fluorescence pattern inside the cell itself. Algal cells in acetone were centrifuged at 1000 rpm for 3 hours to completely remove Chlorophyll-a and the mass was collected after filtering through a sterile membrane filter of 0.45 μm pore diameter. On the other hand, algal cells were kept under stress of fluoride (≥ 15 mg L^{-1}) and incubated for a period of 15 days to have the cells containing completely damaged Chlorophyll-a. An untreated culture (in absence of fluoride) incubated similarly to the treated culture served as a control. Considering its analytical application in real samples, micrographs were also taken for the detection of fluoride (0.01 mg mL^{-1}) amid several other commonly occurring anions (Cl^{-1}, Br^{-1}, I^{-1}, SO_4^{-2}, ClO_4^{-}, CH_3COO^{-}) and cations like Na^{+}, K^{+}, Cr^{+3}, Cu^{+2}, Co^{+2}, Ni^{+2}, Zn^{+2}, Cd^{+2}, Hg^{+2}, Pb^{+2} in their natural contamination concentration (50–300 mg L^{-1})

ranges. Confocal microscopy images were taken at an excitation of 552 nm and emission of 568-597 nm laser sources to find out the role of algal pigments behind the fluorescence pattern inside the cell.

2.4 Systematic studies on luminescence properties: Chlorophyll-a was extracted with 90% acetone [34]**.** A set (five) of fluorescence sample in DMSO was prepared by dissolving extracted Chlorophyll-a. Fluorescence spectra of Chlorophyll-a were recorded on perkinElmer LS-55 spectrofluorometer at its varying concentrations (0.325×10^{-6}-5×10^{-6} (M)). Effect of Rhodamine B (0.2×10^{-6}-0.5×10^{-6} (M) on the fluorescence patteren of Chlorophyll-a at its fixed concentration was investigated. Fluorescence patteren of solution containing Chlorophyll-a and rodamine B at their fixed concentration (0.325×10^{-6} M) was investigated over the range of fluoride concentrations, 0.168×10^{-6} – 0.782×10^{-6} (M). Luminescence properties of all the systems were carried out at an excitation wavelength 330 nm.

2.5 Influence of Fluoride Exposure: Assays were conducted with exponentially growing culture of P. luridum (3 × 104 cells mL^{-1}) in 25 mL of BG 11 (+). Algal suspensions were placed in a set of cuvettes containing fluoride solutions (5 mL) at range of concentrations 10–50 mg L^{-1}. Micrographs of P. luridum (both the pure and algal cells under stressed conditions) at different time intervals (1–14 days) were recorded on an Olympus BX41 epifluorescence trinocular microscope fitted with a digital camera (MC 120 HD at a magnification of 45× 10) to observe any morphological changes.

2.6 Sorption studies: Fluorescence and Confocal microscopic studies indicate definite transport of fluoride inside the algae cells. Systematic investigations were performed (both batch and column method) on sorption (at required time interval to attain equilibrium) of fluoride [(assym. HF_2^-(aq); η =15.21 eV] at different initial concentrations (10–50 mg L^{-1}) over a pH range of 6.5–7.5.

2.6.1 Batch Experiment: Systematic studies on batch equilibrium experiments have been carried out to find the optimum pH, contact time, temperature, and solution concentration for quantitative sorption of fluoride on the surface of biomass. A set of six flasks (250 mL) containing biomass (0.1 g) were

shaken at a constant rate (1000 rpm), allowing sufficient time for adsorption equilibrium. It was assumed that the optimum shaking speed allows all the surface area to come in contact with analyte over the entire period of experiments. The study was carried out at room temperature (27°C) representing environmentally relevant condition.

Adsorption isotherm: 0.1g biomass was taken in 100 mL fluoride solution of different initial concentrations (8-20 mg L^{-1}) at neutral pH. The solutions were stirred at 1000 rpm for 10 min and the amount of fluoride adsored per unit mass, q_e (mg g^{-1}) was computed (eq. 1) [34].

$$q_e = (C_i - C_e)V/m \quad (1)$$

Here, C_i and C_e are initial and equilibrium concentrations (µg mL^{-1}), m is the mass (g) of biosorbent, and V is the analyte volume (mL). Different parameters of the batch experiment are given in Table 1.

The correlation coefficients, R^2 and the residual root mean square error (RMSE) (eq. 2) were used to examine the goodness-of-fit for the applicability of Langmuir (eq. 3) and Freundlich (eq. 4) isotherms [33, 34]. The maximum R^2 and a minimum RMSE value give the applicability of the isotherms.

$$\text{RMSE} = \sqrt{[\frac{1}{m-2}\sum_{i=1}^{m}(q_e - q_{e(t)})^2]} \quad (2)$$

[Where, q_e = the experimental value (average of three determinations), $q_{e(t)}$ = estimate from isotherms for corresponding q_e and m = number of observations].

$$\frac{C_e}{q_e} = \frac{1}{Q_0 b} + \frac{C_e}{Q_0} \quad (3) \quad \& \quad \log q_e = \log K_F + \left(\frac{1}{n}\right)\log C_e \quad (4)$$

Here, q_e is the amount of fluoride sorbed (mg g^{-1}), Q_0 is the monolayer adsorption capacity (mg g^{-1}), b is a constant related to the binding energy for fluoride to algal surface (L mg^{-1}), and C_e is the fluoride concentration at equilibrium (mg L^{-1}). With increase in b, more and more adsorbate gets adsorbed (i.e., $\frac{C_e}{q_e}$ will decrease); which, in turn, decreases the intercept and appreciates Langmuir. The adsorption constants K_F and 1/n in true sense are the measures of adsorption capacity and adsorption intensity, respectively. K_F is an empirical parameter, composed of three components: a binding constant, a term related to the number of adsorption sites, and solution composition. Practically, solution composition is constant for any given water sample. Thus, in practice, only the binding constant and the number of surface sites are the true contributor of K_Fs. Parameter n is a measure of affinity between sorbate and the surface. Sorption ability increases with increase in n [42]. Freundlich 1/n could be estimated based on the structure of the adsorbent cell surface and the density of carboxyl groups on that surface [43].

2.6.2 Column experiments: Batch adsorption equilibrium isotherm studies suggest the maximum sorption capacity for monolayer saturation (Q_0) of the ion exchange material, binding energy of adsorbates to the ion exchange surface (b: mL μM^{-1}), adsorption capacity (K_F) and adsorption intensity (1/n) of the adsorbent. But, it needs repetitive filtrations in both the extraction and elution steps. Column chromatography is an effective alternative.

2.6.2 (i) Preparation of exchanger bed: The columns (0.8 × 28 mL) were packed with inactivated biomass (1g) containing naturally occurring sands and gravels, collected from river side. An aliquot containing fluoride (20 ppm) in raw water at neutral pH was passed through the column containing micro algae; at a flow rate of 4 mL min^{-1}. After extraction, fluoride was stripped with 5 mL 0.005 M $NaNO_3$ and its amount in every 2 mL fraction was determined by ion selective electrode.

2.6.2 (ii) Effect of pH on extraction: pH seems to be the most important parameter in the biosorptive process: it may affect the solution chemistry of adsorbates, activity of the functional groups in the biomass and the competitive ions [44, 45]. Systematic studies at the range of pH 2.5-7.5 were made to find out the effect of pH on sorption of fluoride.

2.6.2(iii) Break through capacity and preconcentration factor: The exchanger bed was thoroughly cleaned with distilled water. Fluoride solution (0.02 mg mL^{-1}) was passed (4 mL min^{-1}) through the column containing 1g of dry biomass. After saturation through extraction, fluoride was eluted with 5 mL 0.005M $NaNO_3$. To find out the effect of foreign ions on retention of fluoride, an analyte solution (100 mL) containing Cl^-, I^-, Br^-, SO_4^{2-}, PO_4^{3-}, ClO_4^-, CH_3COO^- (Na^+/K^+ salts) in their natural contamination range (50-100 mM L^{-1}) was passed through the column at fixed optimum values of all other variables. Now, turning to the application of the developed method for removal of fluoride in real samples, some analyses were performed with various water samples (pond, well and tap water).

2.6.2 (iv) Effect of temperature on sorption: The feed (fluoride: 0.02 mg mL^{-1}) was passed through the exchanger bed (1g biomass) at the temperature range 278 K – 298 K to investigate the involvement of different thermodynamic parameters in the sorption process. From the slope of the linear relationship (y = -3.2763*x* + 13.0222) between 1000/T and log K_d, ΔH has been evaluated (eq. 5) and utilizing the standard van't Hoff equation (eq. 6 and eq. 7) ΔG and ΔS at 300 K were determined [46].

$$\Delta H = -(slope) \times 2.303 \times R \quad (5)$$

$$\Delta G = -2.303 RT \log K_D \quad (6) \qquad \& \qquad \Delta S = \frac{(\Delta H - \Delta G)}{T} \quad (7)$$

Where, R (8.314 J mol^{-1}) is the gas constant.

2.7 Computational studies: Phycocyanobilin2, the fluoride sensing pigment was found to be present in live algae [34]. Consequently, single crystal XRD for the presiced geometry of Phycocyanobilin2-fluoride complex is not possible. So, as an alternative, reliable DFT calculation was performed to achieve the 3D structural configuration of fluoride loaded Phycocyanobilin2. The geometry of the fluoride loaded complex was optimized with Becke's three parameter hybrid exchange functional and Lee–Yange–Parr correlation functional (B3LYP) [47-49] exploiting 6-31+G** basis set. Optimization was carried out without any geometrical constraints. To ensure that the optimized geometries correspond to true minima on potential energy surface, vibrational frequencies were computed using DFT(B3LYP/6-31+G**). All these calculations were carried out using Gaussian 09 package [40].

3. RESULTS AND DISCUSSIONS:

3.1 Physio-chemical properties of the sorbent: P. luridum is a multi celled green algae species. It is filamentous in shape, about 450-600 μM in length and 2-10 μM in diameter (Fig. 1). The SEM images of the loaded and unloaded form (Fig. S1) indicate that the exchange material is porous and fluoride incorporation influences the structure of the material. Microalgae contain i) a relatively high nitrogen content (2–4 wt%) due to the protein component ii) significantly higher amounts of alkali earth metals and accumulated heavy metals iii) a high halogen content (2.5–4.5 wt%) due to its saline environment (mainly associated with Na) iv) moisture content (8-12%), and v) about 1–2 wt % lipid fraction [50]. The pure algae exhibit three majore steps of weight loss (Fig. S2) corresponding to the thermal decomposition (in TGA) of different bio-polymers [50]. The first step (<180 °C) corresponds to dehydration, 2nd step (180–600°C) corresponds to devolatilisation, and a region for the decomposition of mineral oxides occurs at the 3rd step (> 600°C) [50]. The devolatilisation includes the stepwise decomposition of different bio-polymer fractions. The gradual loss in mass above 600 °C may be attributed to decomposition of oxides of mineral components in pure algae [50, 51].

3.2 Detection of fluoride: Fluorescence microscopy became indispensable to the biological sciences because of its high sensitivity, the selectivity with which it could be used to analyze signals, and its non-destructive character, which made it possible to carry out in vivo experiments for real-time analyses [52]. A very weak fluorescence (for autofluorescence pigment, chlorophyll-a) was obtained from pure algae cell and its intensity was not differ noticeably in presence of fluoride (Fig 2(a-b)). But, intense red colored fluorescence images of higher intensity were obtained for Rhodamine B-stained algal cells (Fig. 2c). Recognition of fluoride (at its very trace level: 0.01 mg L^{-1}) was sensitized by an instantaneous yellow fluorescence (Fig. 2(d-f)) and Fig. 3), which glitters on intense red colored area achieved after staining with Rhodamine B, inside the cell. Both the fluoride concentration and contact time gave a positive influence on fluorescence intensity (Fig. 2 and Fig. 3). It does not affected by the presence of foreign ions like Cl^-, I^-, Br^-, SO_4^{2-}, ClO_4^-, CH_3COO^-. This indicates a selective fluoro-complexation with algal pigments. Algae cells with damaged Chlorophyll-a or without Chlorophyll-a also gave the same fluorescence pattern inside the cell (Fig. 4). Outside the cell either Rhodamine B itself or its presence with fluoride does not give any detectable color changes. Consequently, cellular pigments other than Chlorophyll-a of living algae seem to play an anchoring role to make a very high fluorescent sensitive complex (red) with Rhodamine B and subsequently it is able to sense fluoride at trace level by an instantaneous glittering (yellow fluorescence). Confocal microscopic studies on pure algae cells indicate that the Chlorophyll-a pigment residing just beneath the cell surface (0.6-1.0 μm) produces a weak signal consisting of two fluorescence plates (each of 0.3 μm in thickness) only (Fig.5i(a-b)). This result agrees with the fluorescence micrographs (Fig.2(a-b)). On the other hand, Confocal microscopic images of algal cells (either having Chlorophyll-a or not) stained with Rhodamine B, produce a more intense signal for fluoride. Both these sets of images (for having

Chlorophyll-a or not) (Fig. 5 ii(a-n) and Fig. 5 iii(a-l)) consist of about 12-14 fluorescence plates (starting after 7^{th} plates) appear due to some different pigment seated far away (2.1-2.6 μm; within the cell) from the cell surface of the algae. Systematic studies on luminescence properties of three different solution systems in DMSO medium viz. (a) Chlorophyll-a of varying concentration (b) Chlorophyll-a (of fixed concentration: 5×10^{-6} M) containing Rhodamine B of varying concentration and (c) fixed concentration of both Chlorophyll-a and Rhodamin B (5×10^{-6} M and 0.5×10^{-6} M respectively) containing fluoride of varying concentration show that luminescent character (intensity and number/nature of peaks) are of the same order of magnitude for each of the solution system (a, b, c) (Fig. 6). Fluorescence intensity in Fig. 6c was found to be increased little bit (15-18 units only) with appreciable increase in fluoride concentration (7 fold). Thus, practically, fluoride has no influence on chlorophyll-a. It also clearly indicates that interaction between Rhodamin B and Chlorophyll-a is not responsible for more intense coloration of Rhodamin B stained-cell in its fluorescence image (Fig. 2c). It also to be noted that Chlorophyll-a of the fluoride-contaminated microalgae was found to be affected from the 2nd day and gets completely damaged ≥ 12 days at a concentration of fluoride > 15 mg L^{-1} (Fig. 1(b-d)). It indicates a slow kinetics. On the other hand, fluorescence micrographs (Fig. 2, Fig. 3 and Fig. 4) suggest that transport of fluoride inside the algal cell follows a fast kinetics (required time: 10-20 minutes). It reveals that fluoride does not directly interacts with Chlorophyll-a but it favors the proximity of other algal pigments like Phycocyanobilin2 and affects the system. Phycocyanobilin2 is unit protein of Phycobilisome (PBSs) [53] and it is also the light harvesting antenna, connected with the photosystems and transfers light energy to Chlorophyll-a, the photosynthetic light reaction center [54, 55]. Thus, fluoride instanteneously attacks the algal pigments, Phycocyanobilin2 and as a secondary effect, it slowly affects Chlorophyll-a by preventing transfer of light energy. Both chlorophyll-a and Phycocyanobilin2 contains four pyrole rings in their molecular structures (Fig. 7).

Because of its small size and high charge density, among all other anions fluoride has the highest affinity to protons and the ability to interacts hydrogen-containing polar groups such as NH groups [1]. Heterocyclic nitrogens in Chlorophyll-a (Fig. 7a) are tightly bonded with Mg(II) and have not any –NH proton for fluoride binding through H-bondig. On the other hand, Phycocyanobilin2 contains much attackable heterocyclic -NH [6] protons (Fig.7b) in pyrole rings for hydrogen bonding with F^-**;** an established mechanistic path in fluoride sensing [6].

After fluoride sorption, electronic structure of the adsorbent molecule gets disturbed [34, 38, 56, 57]. Consequently, nearly all FTIR bands were shifted after sorption of fluoride. However, the major change was accompanied by the appearance of two new peaks at 1725 cm^{-1} and 2440 cm^{-1} and another extended broad band, appears at 3132-3650 cm^{-1} as well. The strong absorption band (for pure algae) at 3400-3650 cm^{-1} suffers a shift as a broad band (3132-3650 cm^{-1}) [34, 38] in the loaded FTIR spectrum (Fig. S3a), thereby confirming the formation of intramolecular H-bonds in the fluoride extracted species (Fig.S3a). This clearly indicates the involvement of extractor in the fluoride sorption process. To get insight the mechanistic path for fluoride sensing through the interaction of heterocyclic –NH proton of Phycocyanobilin2 by fluoride, standard DFT calculation was made. Three fluorides exist as H-bonded species [H-bond length 80.78 pm for N(5)H---F(86); H-bond length 90.28 and 64.50 pm for N(9)H---F(82)---HO(61); H-bond length 54.43 pm for F(84)----HO(49)] in the DFT optimized fluoride loaded complex (Fig.S4). The computed FTIR (Fig.S3b) spectra of the optimized protein fragment (Phycocyanobilin2), loaded with fluoride show peaks assigned to –NH stretching in NH---F(86) (DFT) at 3191.3 cm^{-1}; Peak at 2447.3 cm^{-1} (DFT) was found to be present for ν(OH) stretching mode in F(84)----HOOC; Peak at 1732.3 cm^{-1} and 3456 cm^{-1} (DFT) was found to be present respectively for ν(NH) bending and ν(NH) stretching in N(9)H---F(82) (DFT); Peak at 1807.8 cm^{-1} (DFT) for ν(OH) bending mode in NH---F(82)----HOOC. This DFT computed FT-IR spectra

rationalize the experimental FT-IR spectral pattern of the loaded extractor [34, 38, and 58]. It confirms the participation of –NH proton in fluoride uptake [Table S1].

All these results, in unison, give a clear verdict that cellular pigments, Phycocyanobilin2 plays an anchoring role to make a very high fluorescent sensitive complex (intense red) with Rhodamine B and subsequently it is able to sense fluoride at trace level by an instantaneous glittering (yellow fluorescence).

And finally as a plausible mechanistic path it may be stated that; a naturally occurring aqua F^--species, [HF_2^-(Assym.): H-F = 49.7 pm, F—F = 197.3 pm, energy = -5398.2 eV and global hardness, η = 15.2 eV], will have a high chance of interaction (through the HSAB pathway [39]) with the -OH of living extractant, P. luridum, at its surface through the formation of H-bond [34]. The surface, being built up of polysaccharides (glucose is the basic unit of polysaccharides: $\eta_{[glucose]}$ = 6.34 eV), makes a weak complex (Scheme 1(a)) with aqua F^--species, [HF_2^- (assym.); $\Delta\eta_{[glucose/HF2^-(assym.)]}$ = 8.87 eV]. This H-bonded species, [Glucose--HF_2^-] leaves a more interactive $[F(aq)]^-$ species (η =7.01 eV). Subsequently, it moves inside and forms a more stable complex in vivo with Phycocyanobilin2 (Scheme 1(b)), having close/comparable hardness ($\eta_{[Phycocyanobilin2]}$ = 2.37 eV and $\Delta\eta_{[F(aq)^-/Phycocyanobilin2]}$ =4.64 eV).

3.3 Preconcentration, separation, recovery and removal of fluoride: Exploiting the weak complexation at the algal surface (Scheme 1(a)), fluoride in real samples may be quantitatively retrieved through selective elution. On the other hand, the more stable complexing ability with Phycocyanobilin2 in vivo patronizes an efficient fluoride-removal-strategy (Scheme 1(b)) in effluent. Thus, along with detection, fluoride sorption for its preconcentration, separation, recovery and removal was also investigated.

3.3.1 Sorption parameters and isotherm equations: Two isotherm (eq. 3 and eq. 4), have been investigated to rationalize the sorption behavior of biomass towards fluoride uptake. The relationships show their applicability for both Langmuir (y = 0.16441x + 1.28757; R = 0.9928; SD = 0.062) and Freundlich (y = 0.36227x + 0.17486; R^2: 0.9859; SD: 0.08) isotherms (Fig. S5). However, the comparable co-relation coefficient and lower RMSE (0.06) (Table 1) suggests the greater acceptability of Freundlich over Langmuir model. Consequently, it agrees with the formation of multilayer by the gradual sorption of analyte (Freundlich) on the adsorbent surface. An attachment of the adsorbate on the surface of the sorbent is not only guided by hard-soft binding, but, also by the physical types of interactions i.e. the sorption process [59, 60]. Here, the adsorbate gets adsorbed at the first layer on the surface by sorts of chemical nature of binding with high Langmuir energy parameter (b: 0.1277 L mg^{-1}). The maximum sorption (Langmuir Q_0: 6.08 mg g^{-1}) is attained at somewhat reduced level to the column break through capacity (Fig. S6), 6.76 mg g^{-1} as is expected and reiterates the formation of multilayer by sorption with high level of Freundlich adsorption capacity (1.49) and adsorption intensity (n = 5.72).

3.3.2 Effect of temperature, pH, volume and flow rate of the influent [fluoride solution, containing common cations/anions as interference] on sorption: The thermodynamic parameters, (ΔH = 0.063 kJ mol^{-1} ; $\Delta G = -1.21$ kJ mol^{-1} and ΔS = 0.06 kJ mol^{-1}) have been calculated from standard thermodynamic relationships (eq. 5, 6 and 7) utilizing the linear regression (y = -3.2763 + 13.0222) for 1000/T vs log K_d (Fig. S7). The sorption occurs instantaneously ($-\Delta G$) and appreciably and produces a very high level of orderd system (low values of + ΔS) through the accumulation of adsorbate on algal surface. Turning to the effect of pH (2.5–7.5) on the sorption of fluoride on algae, we find that it was quantitative at near neutral pH. Complete retention in column was found up to a flow rate of 4 mL min^{-1}. Systematic studies on desorption and reusability of the material show that 5

mL 0.005M $NaNO_3$ quantitatively elute the sorbed fluoride. Sorption-desorption was run on the same column for 3-4 months and up to 70-90 cycles was found to be quantitative.

During our investigation on break-through capacity (BTC) and preconcentration factor (PF), it was found that the leakage of fluoride (0.02 mg mL^{-1}) was started after passing 338 mL (6.76 mg) of analyte solution through the column containing 1g sorbent (Fig. S6). It gives the maximum up take capacity (BTC) 6.76 mg $g^{-1}$of biomass. During this continuous extraction, fluoride has been accumulated gradually on the column from its influent of lower concentration (0.02 mg mL^{-1}) and after elution the effluent (5 mL) was found to be rich with fluoride with higher concentrations (0.6422 mg mL^{-1}). So the method preconcentrates the analyte in the effluent with a factor of 64.2 (95% recovery) on mg levels. Systematic studies on the effect of influent-volume on sorption of fluoride (10 ppm) indicate that a sample volume up to 0.4 L does not influence the preconcentration factor (PF = $\frac{C_f}{C_i} \times recovery(\%)$) and it optimizes at 72 with a recovery of 90%.

In vivo complexation (Scheme 1(b)) was applied in removal-strategy and effect of foreign ions (50-100 mM L^{-1}) was found to be low enough on the removal (> 93%) of fluoride (Table S2) from its synthetic solution (100 mL). Effectiveness of the proposed method was judged by removal of fluoride at its quantitative range (90%) from some real samples (pond, well and tap water) (20 ppm) (Table 2).

4. Conclusions: Cellular pigments, Phycocyanobilin2 of living algae play an anchoring role to make a very high fluorescent sensitive complex (red) with Rhodamine B and subsequently it becomes able to sense fluoride at trace level (0.01 mg L^{-1}) by an instantaneous glittering (yellow fluorescence). It is well below PHS recommended levels for drinking water (0.7−1.2 ppm), placing this probe among the most subtle fluoride sensors reported to date [61]. Fluoride instantaneously attacks the algal pigments,

Phycocyanobilin2 and as a secondary effect, it prevents the transfer of light energy which slowly affects Chlorophyll-a. Algal biomas effectively adsorp fluoride (Langmuir Q_0: 6.08 mg g^{-1}; column BTC: 6.76 mg g^{-1}; adsorption capacity, K_F: 1.4958 and adsorption intensity, n: 5.72) and the process was found to be endothermic, and its spontaneity is attributed to positive change in entropy (ΔH = 0.063 kJ mol^{-1} ; ΔS = 0.06 kJ mol^{-1} and $\Delta G = -1.21$ kJ mol^{-1}).

Acknowledgments:

M. Chatterjee, one of the authors, gratefully acknowledges the experimental assistance for algal detection (Olympus BX41 epifluorescence trinocular microscope fitted with digital camera, Nikon Coolpix 4500) from the Algal research Laboratories, department of Botany, V.B, W.B., India.

Reference:

(1) (a) Beer, P. D.; Gale, P. A.; Anion Recognition and Sensing: The State of the Art and Future Perspectives, *Angew. Chem., Int. Ed*., **2001**, 40, 486-517. (b) Sui, B.; Kim, B.; Zhang, Y.; Frazer, A.; Belfield, K. D.; Highly Selective Fluorescence Turn-On Sensor for Fluoride Detection, ACS Appl. Mater. Interfaces, 2013, 5, 2920−2923 and references there in.

(2) Yang, Z.; Zhang, K.; Gong, F.; Li, S.; Chen, J.; Ma, J. S.; Sobenina, L. N.; Mikhaleva, A. I.; Yang, G.; Trofimov, B. A. A new fluorescent chemosensor for fluoride anion based on a pyrrole-isoxazole derivative. *J. Org. Chem*. **2011**, 7, 46-52.

(3) Ayoob, S.; Gupta, A. K. Fluoride in Drinking Water: A Review on the Status and Stress Effects. Crit. Rev. *Environ. Sci. Technol*. **2006**, 36 (6), 433-487.

(4) Upadhyay, K.; Mishra, R. K.; Kumar, V.; Chowdhury, P. A coumarin based ICT probe for fluoride in aqueous medium with its real application. Talanta, **2010**, 82, 312-318.

(5) (a) Kleerekoper, M. The role of fluoride in the prevention of osteoporosis. *Endocrinol. Metab. Clin. North Am*., **1998**, 27, 441-52

(b) Gessner, B. D.; Beller, M.; Middaugh, J. P.; Whitford, G. M.; Acute fluoride poisoning from a public water system. *N. Engl. J. Med*., **1994**, 330, 95-99.

(6) (a) Cametti, M.; Rissanen, K.; Recognition and sensing of fluoride anion. Chem. Commun., **2009**, 2809-2829. (b) Zhou, Y.; Zhang, J. F.; Yoon, J.; Fluorescence and Colorimetric Chemosensors for Fluoride-Ion Detection. Chem. Rev. 2014, 114, 5511−5571.

(7) Masood, A. K.; Sankar, J.; Exclusive fluoride ion recognition and fluorescence "turn-on" response with a label-free DMN Schiff base. *Analyst*, **2013**, 138, 4760-63. and references there in.

(8) (a) Kubo, Y.; Ishida, T.; Kobayashi, A.; James, T. D. Fluorescent alizarin–phenylboronic acid ensembles: design of self-organized molecular sensors for metal ions and anions, *J. Mater. Chem*., **2005**, 15, 2889-95. (b) Kubo,Y.; Kobayashi, A.; Ishida, T.; Misawa, Y.; James, T. D. Detection of anions using a fluorescent alizarin–phenylboronic acid ensemble. *Chem. Commun*., **2005**, 2846-48.

(c) Xu, Z.; Singh, N. J.; Kim, S. K.; Spring, D. R.; Kim, K. S.; Yoon, Induction-Driven Stabilization of the Anion–π Interaction in Electron-Rich Aromatics as the Key to Fluoride Inclusion in Imidazolium-Cage Receptors. J. *Chem.–Eur. J*., **2011**, 17, 1163-70.

(9) (a) Subodh Kumar,* Vijay Luxami, and Ashwani Kumar, Chromofluorescent Probes for Selective Detection of Fluoride and Acetate Ions, *Org. Lett.,* Vol. 10, No. 24, 2008 (b) Zhao, C. H. Sakuda, E.; Wakamiya, A.; Yamaguchi, S. Highly Emissive Diborylphenylene-Containing Bis(phenylethynyl)benzenes: Structure–Photophysical Property Correlations and Fluoride Ion Sensing. *Chem.–Eur. J.,* **2009**, 15, 10603-12.

(10) (a) Kimm, T. H.; Swager, T. M. You have full text access to this contentA Fluorescent Self-Amplifying Wavelength-Responsive Sensory Polymer for Fluoride Ions. *Angew. Chem*., *Int. Ed.,* **2003**, 42, 4803; (b) Kim S. Y.; Hong, J. I., Chromogenic and Fluorescent Chemodosimeter for Detection of Fluoride in Aqueous Solution. *Org. Lett*., **2007**, 9, 3109-3112. (c) Hu, R.; Feng, J.; Hu, D.; Wang, S.; Li, S.; Li, Y.; Yang, G.; A Rapid Aqueous Fluoride Ion Sensor with Dual Output Modes. *Angew. Chem. Int. Ed*., **2010**, 49, 4915. (d) Sokkalingam, P.; Lee, C. H.; Highly Sensitive Fluorescence "Turn-On" Indicator for Fluoride Anion with Remarkable Selectivity in Organic and Aqueous Media. *J. Org. Chem*., **2011**, 76, 3820-3828. (e) Du, J.; Hu, M.; Fan, J.; Peng, X. Fluorescent chemodosimeters using "mild" chemical events for the detection of small anions and cations in biological and environmental media. *Chem. Soc. Rev*. **2012**, 41, 4511-35. (f) Yang, Y.; Zhao, Q.; Feng, W.; Li, F.; Luminescent chemodosimeters for bioimaging. *Chem. Rev*. **2013**, 113, 192−270.

(11) (a) Hudnall, T. W.; Chiu, C. W.; Gabba¨ı, F. P., Fluoride ion recognition by chelating and cationic boranes. *Acc. Chem. Res*., **2009**, 42, 388; (b) C. R. Wade, A. E. J. Broomsgrove, S. Aldridge and F. P. Gabba¨ı, Fluoride Ion Complexation and Sensing Using Organoboron Compounds. Chem. Rev., **2010**, 110, 3958 (c) J¨akle, F. Advances in the synthesis of organoborane polymers for optical, electronic, and sensory applications. *Chem. Rev*., **2010**, 110, 3985- 4022. (d) F. Pammera and F. J¨akle, 3-Vinylborane-functionalized oligothiophenes: isomer-dependent electronic structure and fluorescence enhancement upon anion binding. Chem. Sci., **2012**, 3, 2598–2606. (e) Swamy, P. C. A.; Mukherjee, S.; Thilagar, P. Dual emissive borane-BODIPY dyads: molecular conformation control over electronic properties and fluorescence response towards fluoride ions. *Chem. Commun*., **2013**, 49, 993-995; (f) Sarkar, S. K.; Mukherjee, S.; Thilagar, P. Going beyond Red with a Tri- and Tetracoordinate Boron Conjugate: Intriguing Near-IR Optical Properties and Applications in Anion Sensing. *Inorg. Chem*. **2014**, 53, 2343−2345.

(12) (a) Sui, B.; Kim, B.; Zhang,Y.; Frazer A.; Belfield, K. D.; Highly Selective Fluorescence Turn-On Sensor for Fluoride Detection. *ACS Appl. Mater*. *Interfaces*, **2013**, 5, 2920–2923; (b) Wang, J.; Yang, L.; Hou, C.; Cao, H. A new N-imidazolyl-1,8-naphthalimide based fluorescence sensor for fluoride detection. *Org. Biomol. Chem*., **2012**, 10, 6271-274. (c) Wang, C.; Li, G.; Zhang, Q. A novel heteroacene, 2-(2, 3, 4, 5-tetrafluorophenyl)-1H-imidazo [4, 5-b] phenazine as a multi-response sensor for F− detection. *Tetrahedron Lett*., **2013**, 54, 2633-36. (d) Yoon, J.; Kim, S. K.; Singh, N. J.; Kim, K. S.; Imidazolium receptors for the recognition of anions. *Chem. Soc. Rev*., **2006**, 35, 355; (e) Jun, E. J.; Xu, Z., Lee, M.; Yoon, A ratiometric fluorescent probe for fluoride ions with a tridentate receptor of boronic acid and imidazolium. *J. Tetrahedron Lett*., **2013**, 54, 2755-58.

(13) Sivaraman, G.; Chellappa, D. Rhodamine based sensor for naked-eye detection and live cell imaging of fluoride ions. *J. Mater. Chem*. *B*, **2013**, 1, 5768-72.

(14) Mohan, D.; Sharma, R.; Singh, V. K.; Steele, P.; Pittman Jr., C. U. Fluoride Removal from Water using Bio-Char, a Green Waste, Low-Cost Adsorbent: Equilibrium Uptake and Sorption Dynamics Modeling. *Ind. Eng. Chem. Res*., **2012**, 51, 900–914.

(15) Ayoob, S.; Gupta, A. K.; Bhat, V. T. A Conceptual Overview on Sustainable Technologies for the Defluoridation of Drinking Water. *Crit. Rev. Environ. Sci*. *Technol*., **2008**, 38, 401-470.

(16) Bhatnagar, A.; Kumar, E.; Sillanp€a€a, M. Fluoride Removal from Water by Adsorption. *A Review. Chem. Eng.J*., **2011**, 171 (3), 811-840.

(17) Das, N.; Pattanaik, P.; Das, R. Defluoridation of Drinking Water Using Activated Titanium Rich Bauxite. *J. Colloid Interface Sci*., **2005**, 292, 1-10.

(18) Fan, X.; Parker, D. J.; Smith, M. D. Adsorption Kinetics of Fluoride on Low Cost Materials. Water Res. 2003, 37, 4929-37.

(19) Yang, C.-L.; Dluhy, R. Electrochemical Generation of Aluminum Sorbent for Fluoride Adsorption. *J. Hazard. Mater*. 2002, B94, 239-252.

(20) Ramos, R. L.; Ovalle-Turrubirates, J.; Sanchez-Castillo, M. A. Adsorption of Fluoride fromAqueous Solution onAluminum-Impregnated Carbon. *Carbon*, **1999**, 37, 609-617.

(21) Ghorai, S.; Pant, K. K., Equilibrium, Kinetics and Breakthrough Studies for Adsorption of Fluoride on Activated Alumina. *Sep. Purif. Technol*., **2005**, 42, 265-271.

(22) Tripathy, S. S.; Bersillon, J.-L.; Gopal, K. Removal of Fluoride from Drinking Water by Adsorption onto Alum-Impregnated Activated Alumina. *Sep. Purif. Technol*., **2006**, 50 (3), 310-17.

(23) Changa, C.-F.; Lin, P.-H.; Holl, W. Aluminum-Type Superparamagnetic Adsorbents: Synthesis and Application on Fluoride Removal. *Coll. Surf. A*, **2006**, 280, 194-202.

(24) Abe, I.; Iwasaki, S.; Tokimoto, T.; Kawasaki, N.; Nakamura, T.; Tanada, S. Adsorption of Fluoride Ions onto Carbonaceous Materials. *J. Colloid Interface Sci*., **2004**, 275, 35-39.

(25) Cengelo glu, Y.; Kır, E. l.; Ers€oz, M., Removal of Fluoride from Aqueous Solution by using Red Mud. *Sep. Purif. Technol*., **2002**, 28, 81-86.

(26) Onyango, M. S.; Kojima, Y.; Aoyi, O.; Bernardo, E. C.; Matsuda, H. Adsorption equilibrium Modeling and Solution Chemistry Dependence of Fluoride Removal from Water by Trivalent-Cation-Exchanged Zeolite F-9., *J. Colloid Interface Sci*., **2004**, 279, 341-50.

(27) Kamblea, S. P.; Jagtap, S.; Labhsetwar, N. K.; Thakare, D.; Godfrey, S.; Devotta, S.; Rayalu, S. S. Defluoridation of Drinking Water using Chitin, Chitosan and Lanthanum-Modified Chitosan. *Chem. Eng. J*., **2007**, 129, 173-180.

(28) Ma, W.; Ya, F.-Q.; Mei Han, R. W., Characteristics of Equilibrium, Kinetics Studies for Adsorption of Fluoride on Magnetic-Chitosan Particle., *J. Hazard. Mater*., **2007**, 143, 296-302.

(29) Reardon, E. J.; Wang, Y. A., Limestone Reactor for Fluoride Removal from Wastewaters. Environ. Sci. Technol., **2000**, 34, 3247-53.

(30) Sinha, S.; Pandey, K.; Mohan, D.; Singh, K. P. Removal of Fluoride from Aqueous Solutions by Eichhornia crassipes Biomass and Its Carbonized Form., *Ind. Eng. Chem. Res*., **2003**, 42, 6911-918.

(31) Li, Y. H.; Wang, S. G.; Zhang, X. F.; Wei, J. Q.; Xu, C. L.; Luan, Z. K.; Wu, D. H. Adsorption of Fluoride from Water by Aligned Carbon Nanotubes. Mater. Res., **2003**, 38, 469.

(32) Leyva-Ramos, R.; Rivera-Utrilla, J.; Medellin-Castillo, N. A.; Sanchez-Polo, M. Kinetic Modeling of Fluoride Adsorption from Aqueous Solution onto Bone Char. Chem. Eng. J. **2010**, 158 (3), 458-467.

(33) Mandal, B. Ghosh, C. U.; Roy, S. Role of river-derived algae on bioaccumulation in fixed bed reactors; a low-cost safe drinking water plant. DWT, 45 (2012) 343-350.

(34) Mandal, B. Mondal, Monalisha, Srivastava, B.; Barman, M. K.; Ghosh, C.; Chatterjee, Mousumi Chromatographic method for pre-concentration and separation of Zn(II) with microalgae and density functional optimization of the extracted species. *RSC Adv*., **2015**, 5, 31205-218.

(35) Volesky, B.; Holan, Z.R.; Biosorption of heavy metals, Biotechnol. Prog., **1995**, 11, 235–250.

(36) Mohan, S. V. Ramanaiah, S.V.; Rajkumar,B.; Sarma, P. N.; Removal of fluoride from aqueous phase by biosorption onto algal biosorbent Spirogyra sp.-IO_2: Sorption mechanism elucidation. J. Hazardous Materials, **2007**, 141, 465–474

(37) Bhatnagar, M.; Bhatnagar, A.; Jha, S. Interactive biosorption by micro algal biomass as a tool for fluoride removal, *Biotechnol. Lett*., **2002**, 24, 1079–1081.

(38) Ghosh, P.; Ray, B. G.; Mukhopadhyay, S. K.; Banerjee, P.; Recognition of fluoride anion at 10 ppm level inside living cell and from fluorine affected tooth and saliva samples, *RSC Advance*, **2015**, 5, 27387-392.

(39) Pearson, R. G. Electronegativity and Hardness: Application to Inorganic Chemistry, *Inorg. Chem*., **1988**, 27, 734–740.

(40) E. Frisc, M. J. Frisch, F. R. Clemente Trucks, G. W.; Gaussian 09, Revision D.01.Gaussian, Inc., Wallingford CT, **2013**.

(41) Gupta, S.; Agrawal, S. C. Survival of blue-green and green algae under stress condition, Folia Microbiol., **2006**, 51(2), 121–128.

(42) Ozer, A., Ozer, D., Dursun, G., Bulak, S., Cadmium(II) adsorption on Cladophora crispata in batch stirred reactors in series., *Waste Management,* **1999**, 19, 233–240.

(43) Chang, H.T., Furuya, E.G., Miura, Y., Noll, K. E., Effect of surface functional groups on Freundlich adsorption isotherm., *Water Science and Technology*, **2000**, 42, 161–166.

(44) Galun, M., Galun, E., Siegel, B. Z., Keller, P., Lehr, H., Siegel, S. M., Removal of metal ions from aqueous solutions by Pencillium biomass: Kinetic and uptake parameters, *Water, Air and Soil Pollution.,* **1987**, 33, 359-371.

(45) Friis, N., Myers-Keith, P. Biosorption of uranium and lead by *Streptomyces longwoodensis*. Biotechnol. Bioeng. **1986**, 28, 21-28.

(46) Mandal, B.; Roy, U. S.; Datta, D. Ghosh, N. Combined Cation-Exchange and Extraction Chromatographic Method of Pre-concentration and Concomitant Separation of Cu(II) with High Molecular Mass Liquid Cation Exchanger after its online detection, *J. Chromatogr. A*, **2011**, 1218, 5644–5652.

(47) (a) Becke**,** A. D. Density-functional exchange-energy approximation with correct asymptotic behavior *Phys. Rev. A: At., Mol., Opt. Phys.,* **1988,** 38, 3098–3100**.** (b) Becke, A. D.; A new mixing of Hartree–Fock and local density-functional theories. *J. Chem. Phys*., **1993**, 98, 1372–1377 (c) Becke, A. D.; Density-functional thermochemistry. III. The role of exact exchange. *J. Chem. Phys*., **1993**, 98, 5648–5652; (d) Lee, C.; Yang, W.; Paar, R. G.; Development of the Colle-Salvetti correlation-energy formula into a functional of the electron density. Phys. Rev. B, **1988**, 37, 785–789.

(48) (a) Hay, P. J.; Wadt, W. R., Ab initio effective core potentials for molecular calculations. Potentials for K to Au including the outermost core orbitals. *J. Chem. Phys*., **1985**, 82, 299–310; (b) Dunning, J.; Hay, J.; Schaefer, H. F. Plenum, Modern Theoretical Chemistry, New York, **1976**, 3, 1.

(49) Hehre, W. J.; Radom, Schleyerand, L. P. V. R.; Pople, J. A. Ab Initio Molecular Orbital Theory, Wiley Interscience, New York, **1986**.

(50) Ross, A. B.; Anastasakis, K.; Kubacki, M.; Jones, J. M. Investigation of the pyrolysis behaviour of brown algae before and after pre-treatment using PY-GC/MS and TGA, *Journal of Analytical and Applied Pyrolysis*. **2009**, 85, 3–10.

(51) Anastasakis, K.; Ross, A. B.; Jones, J. M.; Pyrolysis behaviour of the main carbohydrates of brown macro-algae, *Fuel,* 90, **2011**, 598–607.

(52) Zhang, L.; Gase, K.; Baldwin, I.T.; Gális, I.; Enhanced fluorescence imaging in chlorophyll-suppressed tobacco tissues using virus-induced gene silencing of the phytoene desaturase gene, *BioTechniques*, 48(2), **2010**, 125–133.

(53) Micura, R.; Grubmayr, K. Long-wavelength absorbing derivatives of phycocyanobilin: new structural aspects of phytochrom, Bioorg. Med. *Chem. Lett*., **1994**, 4(21), 2517–2522.

(54) Sidler, W. A.; Phycobilisome and phycobiliprotein structures, in The Molecular Biology of Cyanobacteria, ed. D. A. Bryant, Kluwer Academic Publishers, Dordrecht, **1994**,139–216.

(55) Fujita, Y.; Murakami, A.; Aizawa, K.; Short-term and longterm adaptation of the photosynthetic apparatus: homeostatic properties of thylakoids, in The Molecular Biology of Cyanobacteria, ed. D. A. Bryant, Kluwer Academic Publishers, Dordrecht, **1994**, 677–692.

(56) Srivastava B.; Barman M. K.; Chatterjee, M.; Mandal B.,EBT anchored SiO2 3-D microarray: a simultaneous entrapper of two different metal centers at high and low oxidation states using its highest occupied and lowest unoccupied molecular orbital, respectively. *RSC Adv*., **2015**, 5, 55686-703.

(57) Barman, M. K.; Chatterjee, M.; Srivastava, B.; Mandal, B.; Characterization and Density Functional Theory Optimization of a Simultaneous Binder (FSG-XO) of Two Different Species Exploiting HOMO−LUMO Levels: Photoelectronic and Analytical Applications *J. Chem. Eng. Data*, **2015**, DOI: 10.1021/je501013b.

(58) Camargo, J. A. Fluoride Toxicity to Aquatic Organisms: A Review. Chemosphere. **2003**, 50 (3), 251-64.

(59) Okay, O. S.; Donkin, P.; Peters, L. D.; Livingstone, D. R. The role of algae (Isochrysis galbana) enrichment on the bioaccumulation of benzo [a] pyrene and its effects on the blue mussel Mytilus edulis. *Environ. Pollut*., **2000**, 110 (1), 103−113.

(60) H. Okabayashi, I. Shimizu, E. Nishio, C.J. O'Connor, Diffuse reflectance infrared Fourier transform spectral study of the interaction of 3-aminopropyltriethoxysilane on silica gel. Behavior of amino groups on the surface. *Colloid Polym. Sci*. **1997**, 275, 744-753.

(61) Zhou, X.; Lai, R.; Li, H.; Stains, C. I. The 8-Silyloxyquinoline Scaffold as a Versatile Platform for the Sensitive Detection of Aqueous Fluoride. *Anal. Chem*. **2015**, 87, 4081−4086.

Table 1: Langmuir and Freundlich parameters

[Algae: 0.1 g; sample volume: 100 mL; Temperature: 27 °C; stirring: 1000 rpm]

C_e	q_e (Exp.)	C_e/q_e	q_e (Theoretical)		RMSE	
(mg L^{-1})	(mg g^{-1})	(g L^{-1})	Langmuir	Freundlich	Langmuir	Freundlich
08	3.2000	2.5	3.07355(0.1265)	3.1771(0.0229)	0.09	0.06
10	3.3667	2.9703	3.41103 (-0.04433)	3.4445(0.0778)		
12	3.7651	3.1872	3.68043(0.08467)	3.67978(0.0853)		
14	3.8674	3.6200	3.9005(-0.0331)	3.8909(-0.0235)		
16	4.0794	3.9221	4.08358(-0.0042)	4.0838(-0.0044)		

The differences between theoretical and experimental values for q_e are shown in parenthesis

Table 2: Removal of fluoride [biomass: 1g; Sample volume: 100 mL; Flow-rate: 4 mL mL^{-1}; Temperature: 27 °C; pH of the influent sample: 6.8]

Sample	**Water samples: 100 mL**			
	Anion	**Added (ppm)**	**Found (ppm)**	**Removal (%)**
Pond water	Fluoride	20	1.82	90.9
Well Water	Fluoride	20	1.28	93.6
Tap Water	Fluoride	20	1.54	92.3

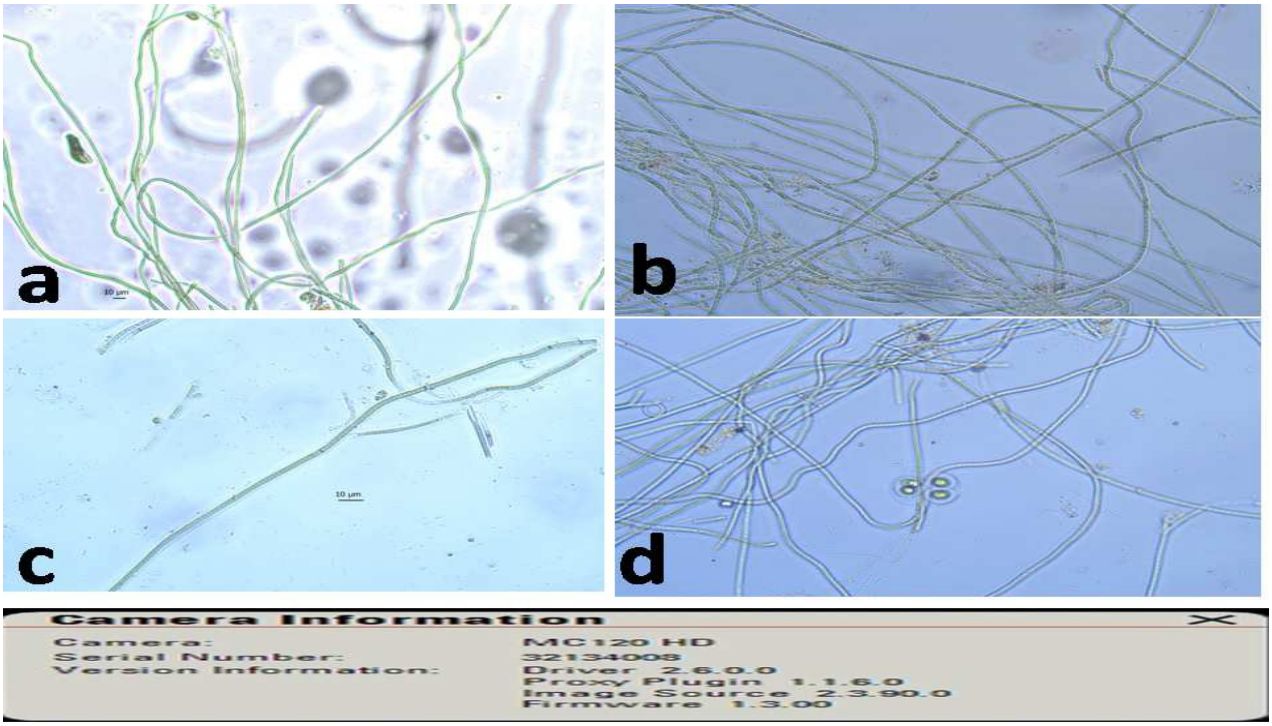

Fig. 1: effect of fluoride (≥ 15 mg L^{-1}) on Chlorophyll-a at different time interval: (a) 24 hours (b) 48-72 hours (c) 72-96 hours and (d) ≥ 8-12 days.

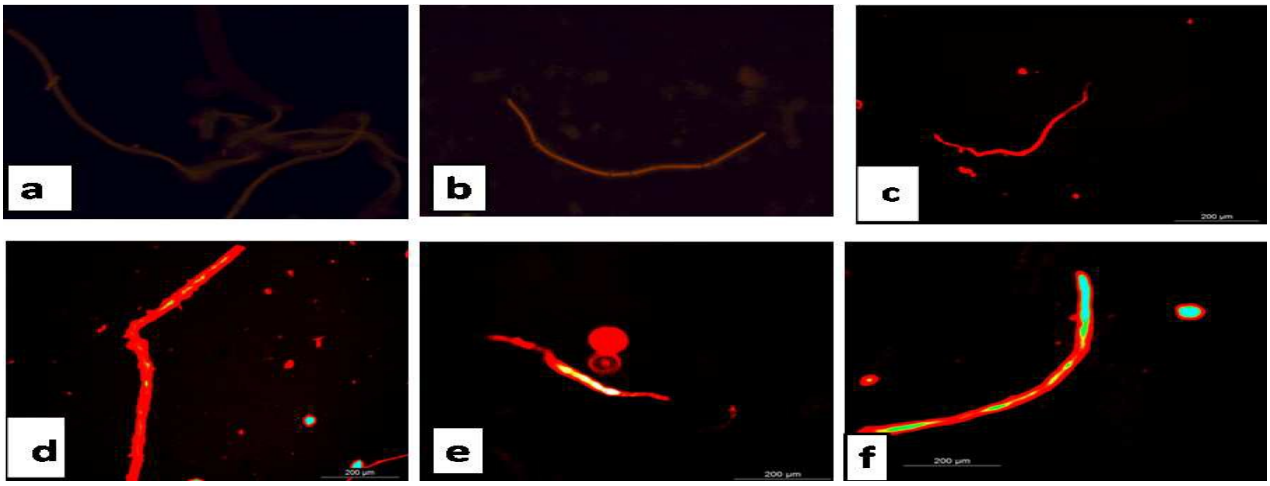

Fig. 2: Fluorescence micrographs of P. luridum in presence of interfering ions like Cl^-, I^-, Br^-, SO_4^{2-}, ClO_4^-, CH_3COO^- (a) pure algae cell (b) pure algae cell in presence of fluoride (c) algae cell, staining with Rhodamine B; (d-f) influence of fluoride concentration on algae cell, staining with Rhodamine B at a constant time interval (10 minutes): (d) 0.01 mg L^{-1}) (e) 0.05 mg L^{-1} and (f) 0.1 mg L^{-1}

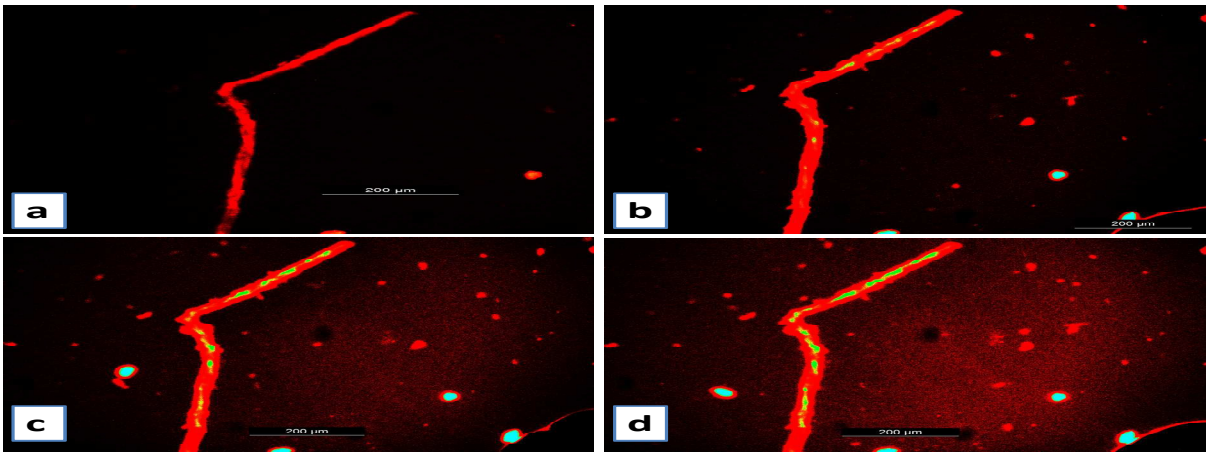

Fig. 3: Fluorescence micrographs of P. luridum in presence of interfering ions like Cl^-, I^-, Br^-, SO_4^{2-}, ClO_4^-, CH_3COO^- (a) algae cell, staining with Rhodamine B; (b-d) influence of fluoride (at constant concentration: 0.01 mg mL^{-1}) on algae, cell staining with Rhodamine B at different time interval: (b) 10 minutes (c) 15 minutes and (d) 20 minutes.

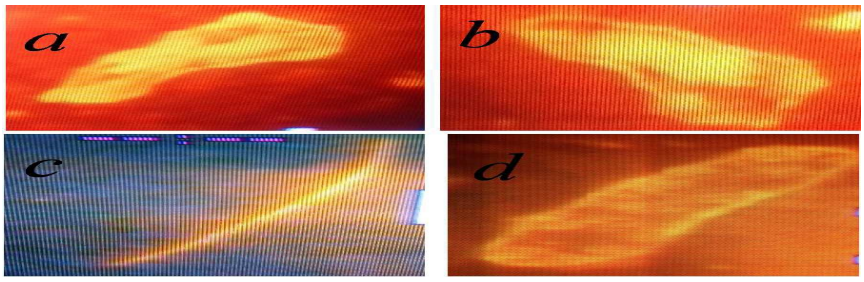

Fig. 4: (a-b) Fluorescence images without Chlorophyll-a at high resolution and (c-d) Fluorescence images in presence of damaged Chlorophyll-a (c) at low and high (d) resolution.

(i)

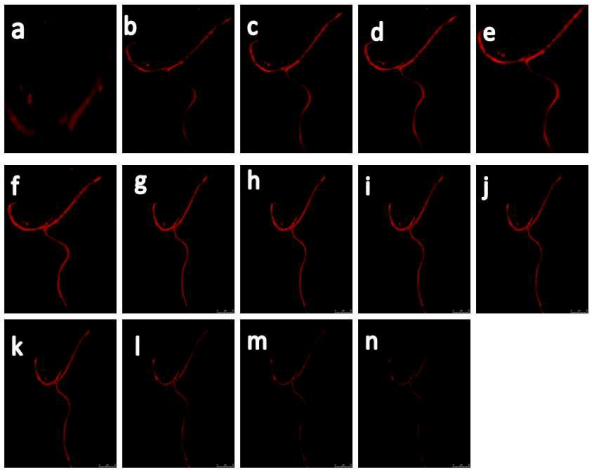

(ii)

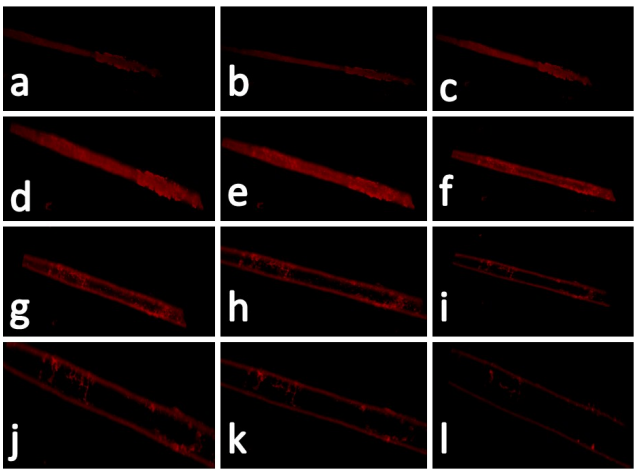

(iii)

Fig. 5: Confocal images (i) fluorescence appears from Chlorophyll-a of pure algae cells; (ii) Chlorophyll-a containing algae cells, stained with Rhodamine B and (iii) Chlorophyll-a free algae cells, stained with Rhodamine B; Both (ii) and (iii) comprising of 12-14 fluorescence plates (a-n and a-l; 0.3 μm in thickness of each); Intensity is gradually increases, approaches a maxima at (g/e); then gradually diminishes and reaches a minima at (n/l).

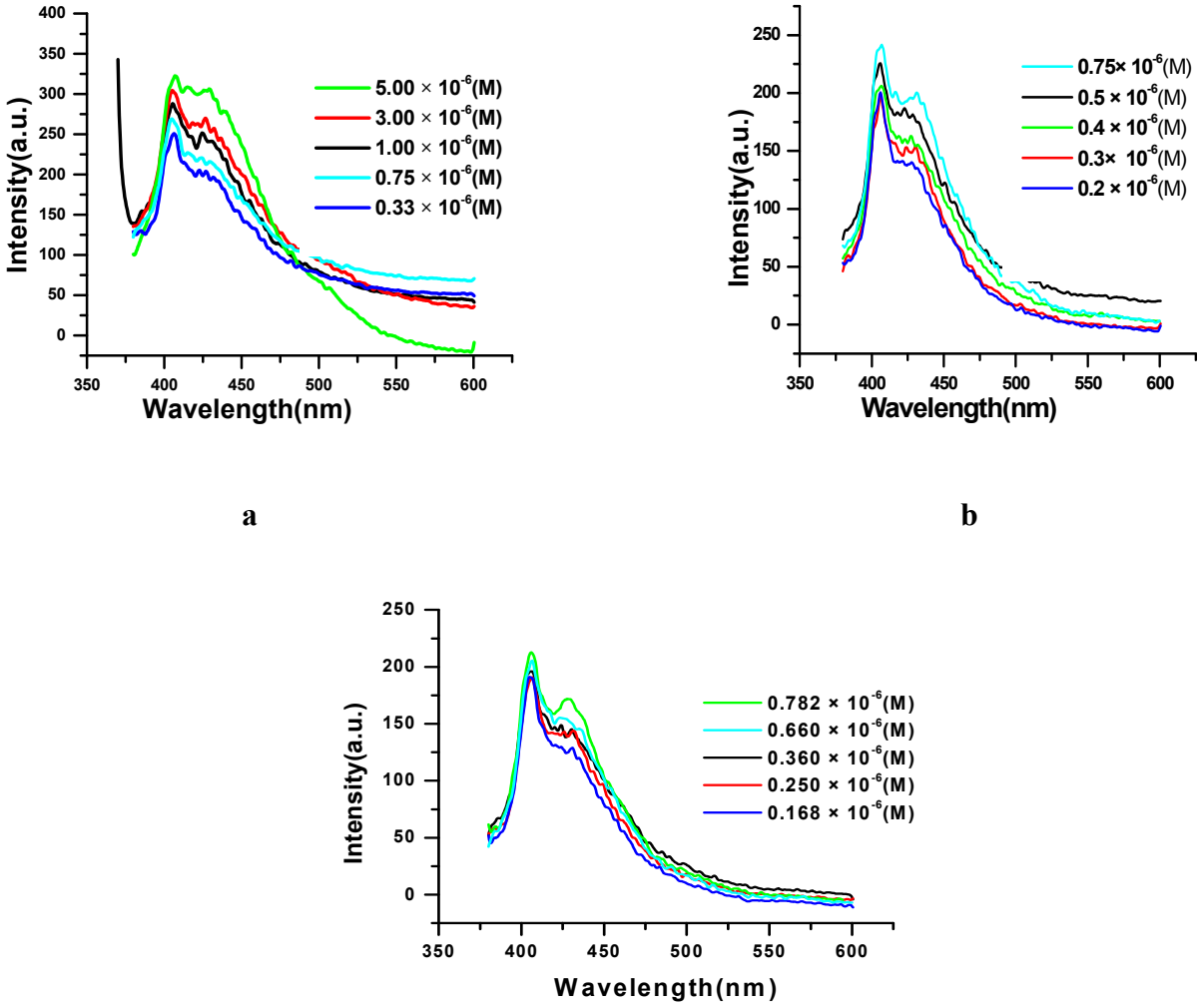

Fig. 6: Luminescent properties of (a) Chlorophyll-a of varying concentration (b) Chlorophyll-a (5×10^{-6} M) containing Rhodamine B of varying concentration (c) fixed concentration of both Chlorophyll-a and Rhodamine B (respectively 5×10^{-6} M and 0.5×10^{-6} M) containing fluoride of varying concentration; Excitation wavelength: 330 nm; Solvent: DMSO

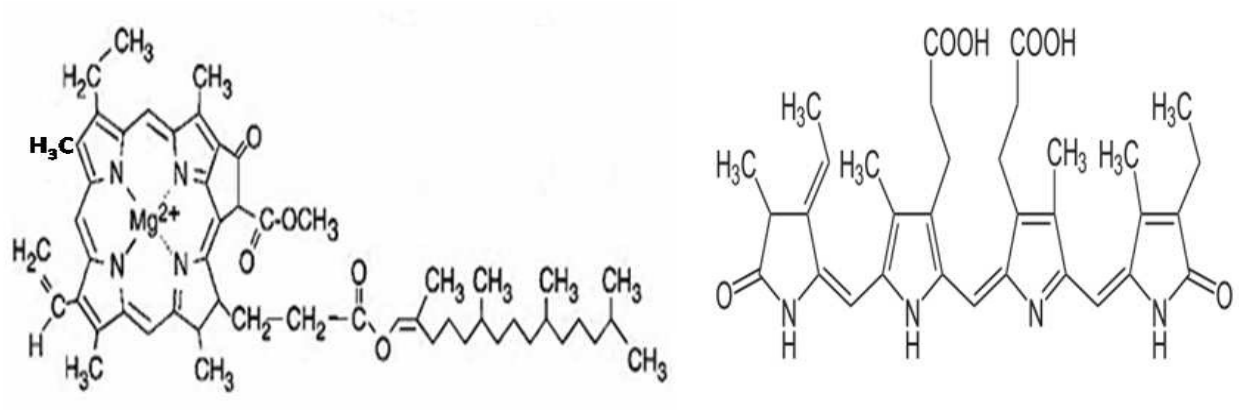

a **b**

Fig. 7: a) Chlorophyll-a and b) Phycocyanobilin2

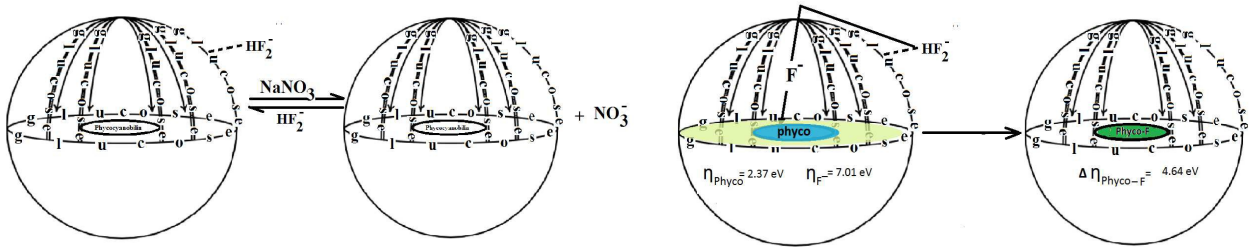

a **b**

Scheme 1: (a) Assym. HF_2^- (η: 15.21 eV)-surface glucose (η: 6.34 eV) weak complexation (Δη: 8.87 eV) and (b) F^- (η: 7.01 eV)-Phycocyanobilin2 (η: 2.37 eV) strong complexation (Δη: 4.64 eV) inside the living cell

Graphical Abstract